Journal of Ceramic Processing Research. Vol. 12, No. 2, pp. 165~168 (2011)

J O U R N A L O F
Ceramic Processing Research

Properties and rapid consolidation of nanostuctured MgO by high frequency induction heated sintering

Hui-Soo Jun[a], In-Yong Ko[a], Jin-Kook Yoon[b], Jung-Mann Doh[b], Kyung-Tae Hong[b], Sang-Hoon Lee[c] and In-Jin Shon[a,d,*]

[a]*Division of Advanced Materials Engineering and the Research Center of Advanced Materials Development, Engineering College, Chonbuk National University, 561-756, Republic of Korea*

[b]*Functional Materials Center, Korea Institute of Science and Technology, PO Box 131, Cheongryang, Seoul 130-650, Republic of Korea*

[c]*New & Renewable Energy Division, Korea Institute of Energy Technology Evaluation & Planning*

[d]*Department of Hydrogen and Fuel Cells Engineering, Specialized Graduate School, Chonbuk National University, 561-756, Republic of Korea*

The rapid sintering of nanostuctured MgO materials in a short time was investigated with a high-frequency induction heating sintering process. A dense nanostructured MgO material with a relative density of up to 99.8% was produced with simultaneous application of 80 MPa pressure and an induced current of with an output of total power capacity (15 kW) within 2 minutes. The effect of the ball milling time on the sintering behavior, grain size and mechanical properties of binderless MgO was investigated. The grain size of sintered MgO decreased with an increase in the milling time. Also the Vickers hardnesses of the MgO with ball milling for 0, 1, 4 and 10 h were 362, 412, 536 and 654 kg/mm^2, respectively.

Key words: Sintering, MgO, Nanostructured material, Powder metallurgy.

Introduction

MgO is widely used in the steel industry or in non-ferrous metallurgical applications under severe conditions [1]. The lifetime of MgO is curtailed by a combined attack of corrosion and mechanical erosion. Refractory wear is very often found to be the most serious at the interface of melt wetted lining areas [2, 3]. To improve its wear property, the approach commonly utilized has been the addition of a second phase to form composites and to make nanostructured materials.

Nanocrystalline materials have received much attention as advanced engineering materials with improved physical and mechanical properties [4, 5]. As nanomaterials possess high strength, high hardness, excellent ductility and toughness, much attention has been paid to the application of nanomaterials [6, 7]. In recent days, nanocrystalline powders have been developed by a thermochemical and thermomechanical process named the spray conversion process (SCP), co-precipitation and high energy milling [8-10]. However, the grain size in sintered materials becomes much larger than that in pre-sintered powders due to a rapid grain growth during a conventional sintering process. Therefore, even though the initial particle size is less than 100 nm, the grain size increases rapidly up to 500 nm or larger during conventional sintering [11]. So, controlling grain growth during sintering is one of the keys to the commercial success of nanostructured materials. In this regard, the high frequency induction heated sintering method (HFIHS) which can make dense materials within 2 minutes has been shown to be effective in achieving this goal [12-15].

In this study, we investigated the sintering of MgO without the use of a binder by the HFIHS method. The goal of this research is to produce dense nano-grained binderless MgO material. In addition, we also studied the effect of the initial particle size on the sintering behavior and mechanical properties of binderless MgO.

Experimental procedure

The MgO powder with a grain size of < 1 μm and 99% purity used in this research was supplied by Aldrich. The powder was first milled in a high-energy ball mill (Pulverisette-5 planetary mill) at 250 rpm for various periods of time (0, 1, 4, 10 h). Tungsten carbide balls (8.5 mm in diameter) were used in a sealed cylindrical stainless steel vial under an argon atmosphere. The weight ratio of balls-to-powder was 30 : 1. Milling resulted in a significant reduction of the grain size. The grain sizes of the MgO was calculated from the full width at half-maximum (FWHM) of the diffraction peak by Suryanarayana and Grant Norton's formula [16] :

$$B_r(B_{crystalline} + B_{strain})\cos\theta = k\lambda/L + \eta\sin\theta \quad (1)$$

where B_r is the full width at half-maximum (FWHM) of

*Corresponding author:
Tel : +82-63-270-2381
Fax: +82-63-270-2386
E-mail: ijshon@chonbuk.ac.kr

the diffraction peak after instrumental correction; $B_{crystalline}$ and B_{strain} are the FWHM caused by small grain size and internal stress, respectively; k is a constant (with a value of 0.9); λ is the wavelength of the X-ray radiation; L and η are the grain size and internal strain, respectively; and θ is the Bragg angle. The parameters B and B_r follow Cauchy's form with the relationship: $B = B_r + B_s$, where B and B_s are the FWHM of the broadened Bragg peaks and the standard sample's Bragg peaks, respectively.

The powders were placed in a graphite die (outside diameter, 40 mm; inside diameter, 10 mm; height, 40 mm) and then introduced into the high-frequency induction heating sintering (HFIHS) apparatus shown schematically in references [12-15]. The HFIHS apparatus includes a 15 kW power supply which provides an induced current through the sample, and a 50 kN uniaxial press. The system was first evacuated and a uniaxial pressure of 80 MPa was applied. An induced current was then activated and maintained until the densification rate was negligible, as indicated by the real-time output of the shrinkage of the sample. The shrinkage was measured by a linear gauge measuring the vertical displacement. The HFIHS can be controlled in two ways: by temperature control or by output control. The latter was chosen to investigate the effect of the output of the total power, given that the induced current level has a direct effect on the rate of heating and on the maximum temperature. The output level was 80% output of the total power. Temperatures were measured by a pyrometer focused on the surface of the graphite die. At the end of the process, the induced current was turned off and the sample cooled to room temperature. The process was carried out under a vacuum of 5.33 Pa.

The relative density of the sintered sample was measured by the Archimedes method. Microstructural information was obtained from product samples, which had been polished and etched using thermal etching for 1 h at 1100 °C. Compositional and microstructural analyses of the products were made through X-ray diffraction (XRD), scanning electron microscopy (SEM) with energy dispersive X-ray spectroscopy (EDS) and a field emission scanning electron microscope (FE-SEM). Vickers hardness was measured by performing indentations at a load of 10 kg with a dwell time of 15 s.

Results and Discussion

Fig. 1 shows X-ray diffraction patterns of the MgO powder after various milling times. The full width at half-maximum (FWHM) of the diffraction peak is wider with milling time due to strain and refinement of the powder. Fig. 2 shows plots of $B_r\cos\theta$ versus $\sin\theta$ of MgO milled for various times to calculate particle sizes from the XRD data. The average grain sizes of the MgO milled for 1, 4 and 10 h determined by Suryanarayana and Grant Norton's formula were about 25 nm, 20 nm and 15 nm, respectively.

SEM images of MgO powder as a function of milling time are shown in Fig. 3. MgO powder without milling has an angular shape but the MgO powder has a round shape and refinement by milling. The variations of the shrinkage displacement and temperature with the heating time for 80% of the total output power capacity (15 kW) during the sintering of the high energy ball milled MgO under a pressure of 80 MPa are shown in Fig. 4. In all cases, the application of the induced current resulted in shrinkage due to consolidation. The shrinkage initiation temperature varied from 820 to 920 K depending on the milling time.

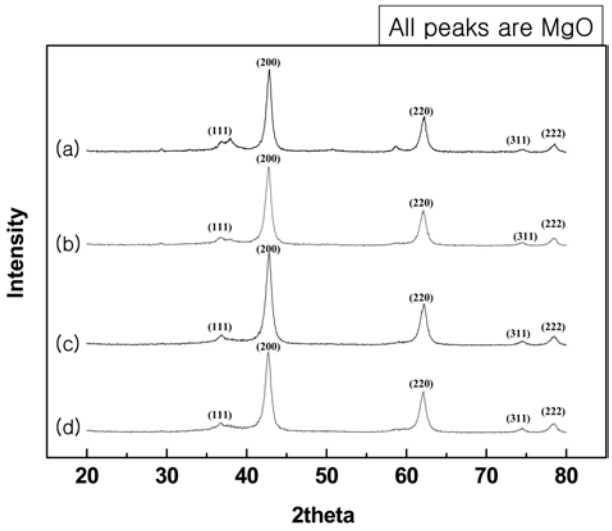

Fig. 1. X-ray diffraction patterns of the MgO powder after various milling time : (a) 0, (b) 1, (c) 4, and (d) 10 h.

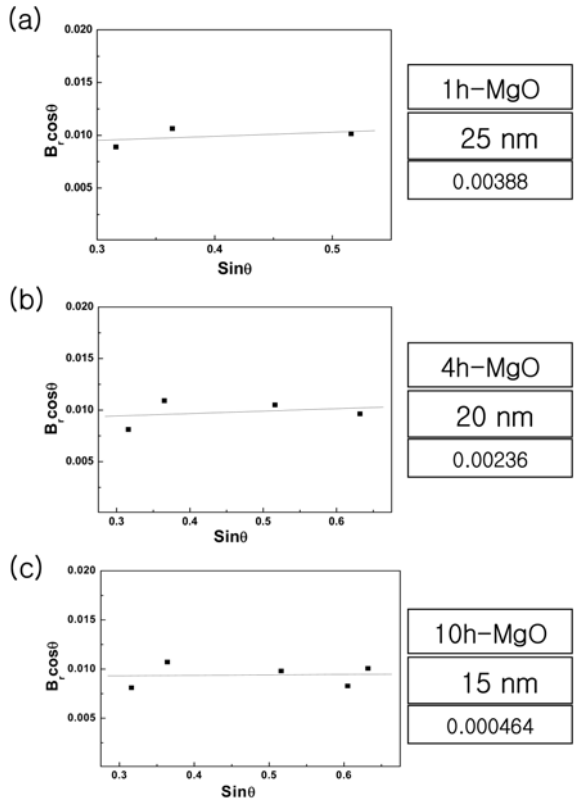

Fig. 2. Plots of B_r ($B_{crystalline} + B_{strain}$) cosθ versus sinθ for various milled MgO powders : (a) 1, (b) 4, and (c) 10 h.

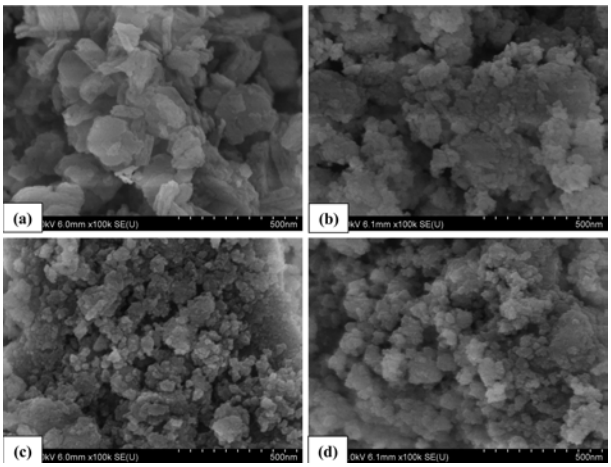

Fig. 3. FE-SEM images of MgO powders with milling times : (a) 0, (b) 1, (c) 4, and (d) 10 h.

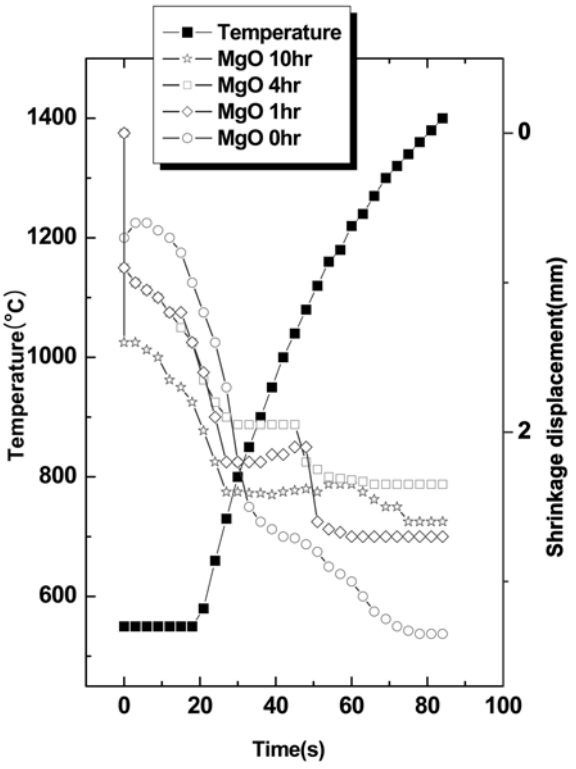

Fig. 4. Variations of temperature and shrinkage with heating time during the sintering of binderless MgO with milling times of 0, 1, 4, and 10 h.

The temperature at which shrinkage started decreased with increasing milling time, and the high energy ball milling affected the rate of densification and the final density, as will be discussed below. A high-energy ball milling treatment allows the control of the formation of a compound by fixing the MgO powder microstructure. Indeed, high-energy ball milling produces finer crystallites, strain and defects. Therefore, the consolidation temperature decreases with the milling time because the driving force for sintering and contact points of particles for atomic diffusion increases. Fig. 5 shows the XRD patterns of MgO

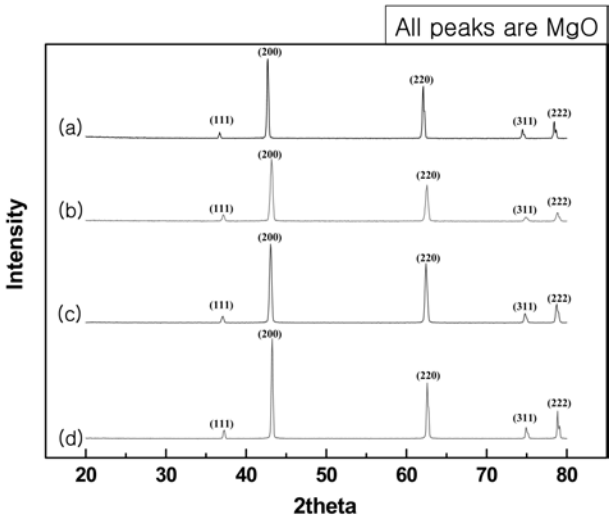

Fig. 5. XRD patterns of binderless MgO sintered from various milled powders : (a) 0, (b) 1, (c) 4, and (d) 10 h.

sintered for all four powders used in this study. All peaks are MgO. Plots of B_r ($B_{crystalline} + B_{strain}$) cosθ versus sinθ in Suryanarayana and Grant Norton's formula [16] are shown in Fig. 6. The average grain sizes of the MgO calculated from the XRD data were about 94, 66, 52 and 47 nm for the samples with milling times of 0, 1, 4, and 10 h and their corresponding densities were approximately 98. 99, 99 and 99.8%, respectively. Thus, the average grain size of the sintered MgO is not greatly larger than that of the initial powder, indicating the absence of substantial grain growth during sintering. This retention of the grain size is attributed to the high heating rate and the relatively short term exposure of the powders to the high temperature. As the initial particle size of the MgO powder increased, the porosity also increased. FE-SEM images of MgO sintered from powder milled for various times are shown in Fig. 7. From the figures, grains have a round shape in MgO sintered unmilled powder but grains have a lamellar shape in MgO sintered milled powders, and the MgO consists of nanocrystallines.

The role of the current (resistive or inductive) in sintering and or synthesis has been the focus of several attempts aimed at providing an explanation to the observed enhancement of sintering and the improved characteristics of the products. The role played by the current has been variously interpreted, the effect being explained in terms of a rapid heating rate due to Joule heating, the presence of a plasma in the pores separating powder particles, and the intrinsic contribution of the current to mass transport [17-20].

Vickers hardness measurements were performed on polished sections of the MgO samples using a 10 kg load and 15 s dwell time. The Vickers hardnesses of the MgO with ball milling for 0, 1, 4 and 10 h were 362, 412, 536 and 654 kg/mm^2, repectively. The hardnesses of MgO sintered from MgO powder increased with an increase in the milling time due to the refinement of the grain size. Fracture toughness could not be calculated from crack length

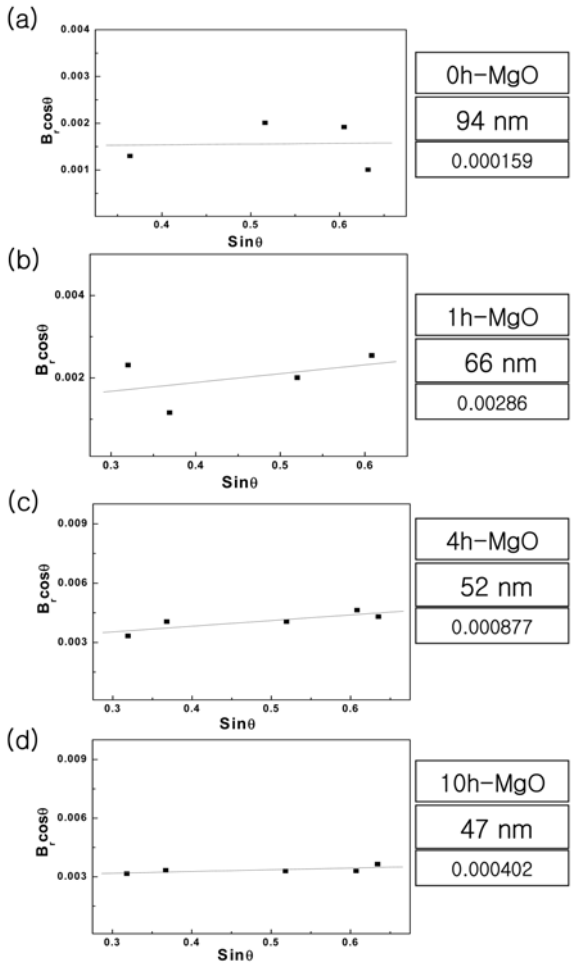

Fig. 6. Plots of B_r ($B_{crystalline} + B_{strain}$) cosθ versus sinθ for MgO sintered from various milled powders : (a) 0, (b) 1, (c) 4, and (d) 10 h.

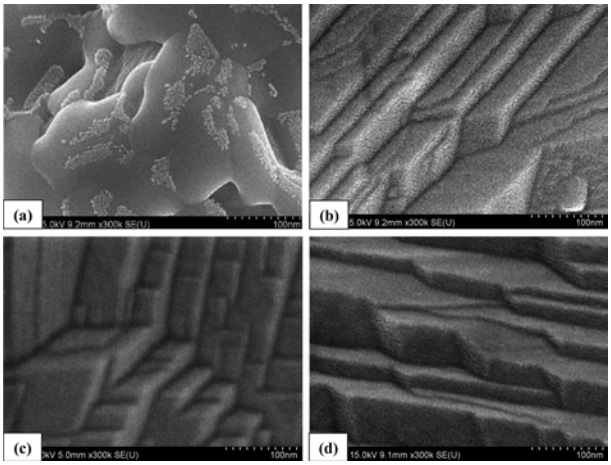

Fig. 7. FE-SEM images of MgO sintered from various milled powders : (a) 0, (b) 1, (c) 4, and (d) 10 h.

because radial cracks did not emanate from the corners of the indents.

Summary

Using the new rapid sintering method, HFIHS, the densification of binderless MgO was accomplished using powder initially refined by high energy ball milling. The consolidation temperature decreased with milling time because the driving force for sintering and contact points of powder particles for atomic diffusion increased. The average grain sizes of the MgO were about 94, 66, 52 and 47 nm for the samples with milling times of 0, 1, 4, and 10 h and their corresponding densities were approximately 98. 99, 99 and 99.8%, respectively. The hardnesses of MgO sintered from the MgO powder increased with an increase in the milling time due to the refinement of the grain size.

Acknowledgment

We are grateful for the financial support from the Korea Institute of Science and Technology, which was provided through the program for study on Development of Surface Treatment for Light Metals.

References

1. R.K. Sauerbrey, G. Mori. Ch. Majcenovic and H. Harmuth, Corrosion Science 51 (2009) 1-5.
2. Z.-Y. Chen, China's Refract. 3 (1994) 3-9.
3. L.B. Khoroshavin and V.B. Shcherbatskii, Refract. Ind. Ceram. 46[5] (2005) 344-351.
4. M. Sherif El-Eskandarany, J. Alloys & Compounds 305 (2000) 225-238.
5. L. Fu, L.H. Cao and Y.S. Fan, Scripta Materialia 44 (2001) 1061-1068.
6. K. Niihara and A. Nikahira, Advanced structural Inorganic Composite, Elsevier Scientific Publishing Co., Trieste, Italy, 1990.
7. S. Berger, R. Porat and R. Rosen, Progress in Materials 42 (1997) 311-320.
8. Z. Fang and J.W. Eason, Int. J. of Refractory Met. & Hard Mater 13 (1995) 297-303.
9. A.I.Y. Tok, L.H. Luo and F.Y.C. Boey, Matrials Science and Engineering A 383 (2004) 229-234.
10. I.J. Shon, D.K. Kim, I.Y. Ko, J.K. Yoon and K.T. Hong, Materials Science Forum 534-536 (2007) 525-528.
11. M. Sommer, W.D. Schubert, E. Zobetz and P. Warbichler, Int. J. of Refractory Met. & Hard Mater 20 (2002) 41-50.
12. H.C. Kim, D.Y. Oh, J. Guojian and I.J. Shon, Mater. Sci. Eng. A 368 (2004) 10-17.
13. H.C. Kim, D.Y. Oh and I.J. Shon, Int. J. Refract. Metals & Hard Mater. 22 (2004) 197-203.
14. D.Y. Oh, H.C. Kim, J.K. Yoon and I.J. Shon, J. Alloys & Compounds 386 (2005) 270-275.
15. H.C. Kim, D.Y. Oh and I.J. Shon, Int. J. Refract. Metals & Hard Mater. 22 (2004) 41-49.
16. C. Suryanarayana and M. Grant Norton, X-ray Diffraction A Practical Approach, Plenum Press, New York, 1998.
17. Z. Shen, M. Johnsson, Z. Zhao and M. Nygren, J. Am. Ceram. Soc. 85 (2002) 1921-1927.
18. J.E. Garay, U. Anselmi-Tamburini, Z.A. Munir, S.C. Glade and P. Asoka- Kumar, Appl. Phys. Lett. 85 (2004) 573-575.
19. J.R. Friedman, J.E. Garay, U. Anselmi-Tamburini and Z.A. Munir, Intermetallics. 12 (2004) 589-597.
20. J.E. Garay, J.E. Garay, U. Anselmi-Tamburini and Z.A. Munir, Acta Mater., 51 (2003) 4487-4495.